ELSEVIER

Physica C 377 (2002) 547–552

PHYSICA C

www.elsevier.com/locate/physc

Comparative study on the transport critical current density of Bi-2223 and Tl-1212 Ag-sheathed superconductor tapes in low magnetic fields

K.T. Lau, S.K. Chen, R. Abd-Shukor *

School of Applied Physics, Universiti Kebangsaan Malaysia, 43600 Bangi, Selangor Darul Ehsan, Malaysia

Received 25 June 2001; received in revised form 4 December 2001; accepted 12 December 2001

Abstract

High-T_c superconductor tapes with nominal compositions of $Bi_{1.8}Pb_{0.4}Sr_2Ca_{2.2}Cu_3O_{10-x}$ (Bi-2223) and (Tl,$Cr_{0.15}$)-$Sr_2(Ca_{0.9},Pr_{0.1})Cu_2O_{7-x}$ (Tl-1212) were fabricated using the powder-in-tube method. The $T_{c\,zero}$'s of the tapes, which were subjected to various thermo-mechanical treatments, ranged from 100–103 K for the Bi-2223/Ag tapes and 84–86 K for the Tl-1212/Ag tapes. Their transport critical current densities in low magnetic fields (0.15 T) were compared. All the tapes are dominated by weak links where this is more severe in the Tl-1212/Ag tapes. No significant anisotropic transport properties were observed in Tl-1212/Ag tapes when the magnetic field was applied perpendicular or parallel to the tape plane (i.e. $J_c(H_\perp)/J_c(H_\parallel) = 0.75$–$1.0$). The Bi-2223/Ag tapes however show a pronounced anisotropic transport properties in applied magnetic field (i.e. $J_c(H_\perp)/J_c(H_\parallel) = 0.15$–$0.65$). This can be associated with the microstructural difference between these two types of tapes. Scanning electron micrographs reveal the slightly aligned grains in the Bi-based tapes while randomly orientated grains were observed in the Tl-based tapes.

PACS: 74.50; 74.72F; 74.72H
Keywords: Anisotropic current density; Strong links; Tapes

1. Introduction

Since early 1990s, much effort has been focused on developing and improving the usage of high temperature superconductors (HTSC) for power applications. Processing of HTSC materials exploiting the powder-in-tube (PIT) method has been one of the commonly used techniques for fabrication of HTSC wires or tapes. However, the prospect of the application of HTSC tapes are strongly hampered by several factors such as Josephson weak links and weak pinning capability especially for Bi-2223/Ag and Bi-2212/Ag tapes.

Attempts in producing Bi-based HTSC tapes with excellent properties have yielded somewhat satisfying results [1–5]. Although the Bi-based HTSC tapes showed extremely weak pinning properties at liquid nitrogen temperature [6–8], it has been successfully used to form long-length HTSC tapes for practical applications compared to other HTSC materials. On the other hand, high

* Corresponding author. Tel.: +60-3-89292904; fax: +60-3-89293777.
E-mail address: ras@pkrisc.cc.ukm.my (R. Abd-Shukor).

0921-4534/02/$ - see front matter
PII: S0921-4534(01)01316-8

critical current densities have been achieved in Tl-based HTSC tapes with flexible long-length scale using various compositions and thermo-mechanical treatments [9–13]. The Tl-1212 system, which belong to single layer Tl–O materials, display favorable irreversibility field compared to double insulating layer systems such as Tl-2212 and Bi-2223 [14,15]. Ren and Wang [16] reported that the Tl-1212 tapes demonstrate better pinning characteristic than the Tl-1223 tapes. Moreover, the Cr-doped Tl-1212 bulk and Ag-sheathed tapes also show high T_c's values above 100 K [17,18].

It is interesting to investigate the transport properties of Bi- and Tl-based HTSC tapes in magnetic field. In this paper we compare the transport properties of Bi-2223 and Tl-1212 Ag sheathed superconducting tapes in applied magnetic fields from 0–0.15 T. The magnetic field dependence of the critical current density (J_c) is useful in characterizing HTSC tapes because it does not depend on possible microcracks and gives an idea of the granularity as well as the local texturing condition [19]. Critical temperatures ($T_{c\,zero}$'s) as well as the micrograph from the scanning electron microscope (SEM) are also presented.

2. Experimental details

$Bi_{1.8}Pb_{0.4}Sr_2Ca_{2.2}Cu_3O_{10-x}/Ag$ (Bi-based tapes) and $(Tl,Cr_{0.15})Sr_2(Ca_{0.9}Pr_{0.1})Cu_2O_{7-x}/Ag$ (Tl-based tapes) tapes were fabricated using the PIT method. Cr is substitute in the Tl-1212 to enhance its transition temperature [17] while Pr is partially substituted for Ca to enhance the formation of the 1212 phase. Powders with starting compositions as mentioned above were prepared by conventional solid-state reaction. For Bi-based tapes, the superconductor powders consist of the 2212 phase as majority phase with the 2223 phase and other secondary phases as minorities. For the Tl-based tapes, the majority phase is the 1212 phase with the 1201 phase as minority. The volume fraction of each phase in both powders was estimated by taking the ratio of the highest peak of the XRD-patterns for one phase with respect to the other. Both powders were fine ground before being packed into a Ag tube of 6.0 mm outer diameter and 4.5 mm inner diameter. The tube was groove rolled, drawn to 1 mm outer diameter and then rolled into tape form. Rolling cylinders of 20 mm in diameter and a rolling speed of about 0.6 m/min were used. The tapes were then cut into small sections (3 cm each) before thermo-mechanical treatments. Both Bi- and Tl-based tapes were divided into three groups each labeled as Bi-A, Bi-B, Bi-C and Tl-A, Tl-B, Tl-C, respectively, and then subjected to different thermo-mechanical treatments as summarized in Table 1. The final thickness of the processed tapes in each group is also included in Table 1.

The phases in the tapes were identified through XRD pattern using a Siemens D5000 diffractometer with Cu-K_α as a radiation source. A Philips

Table 1
Summary of the various thermo-mechanical treatments applied to the tapes with their $T_{c\,zero}$, J_c and final thickness of processed tapes

Sample	1st heating	Intermediate deformation	2nd heating	Heating environment	$T_{c\,zero}$ (K)	J_c at 77 K and self-field (A cm^{-2})	Final thickness of processed tapes (mm)
Bi-2223 tapes							
Bi-A	845 °C × 50 h	Rolling	845 °C × 50 h	Air	103	5310 ± 200	0.22
Bi-B	845 °C × 150 h	–	–	Air	100	1370 ± 100	0.32
Bi-C	850 °C × 50 h	–	–	Air	100	1090 ± 60	0.32
Tl-1212 tapes							
Tl-A	820 °C × 15 min	Rolling	910 °C × 1 h	O_2	86	1020 ± 80	0.12
Tl-B	820 °C × 15 min	Rolling	910 °C × 40 min + 840 °C × 2 h	O_2	86	657 ± 80	0.12
Tl-C	820 °C × 15 min	(Pressing: pressure = 0.15 GPa)	910 °C × 1 h	O_2	84	3060 ± 100	0.25

XL-30 SEM was used to observe the microstructures of the samples. Critical temperature ($T_{c\,zero}$) of the tapes was measured using a dc four-probe technique. Transport critical current density (J_c) measurements were carried out at liquid nitrogen temperature using a dc four-probe technique with 1 μV/cm criterion in magnetic fields varying from 0 to 0.15 T. Magnetic fields (H) were applied perpendicular to the current flow direction, parallel ($H_\parallel$) and perpendicular ($H_\perp$) to the tape plane.

3. Results and discussion

XRD analysis shows the existence of mixed phases of 2223 and 2212 in Bi-based tapes and a majority of the 1212 phase was observed in Tl-based tapes. Secondary phases in both types of tapes may act as flux pinning centers [20]. The measured $T_{c\,zero}$'s are in the range 100–103 K for the Bi-based tapes and 84–86 K for the Tl-based tapes as listed in Table 1 together with the achieved J_c's. Typical measurements for $T_{c\,zero}$ are shown in Fig. 1.

Fig. 2 shows $\log[J_c(H)/J_c(H = 0\ \mathrm{T})]$ versus H for Bi-based tapes with H parallel ($H_\parallel$) and perpendicular ($H_\perp$) to the tape plane. J_c initially decreases rapidly with $H_\parallel$ and $H_\perp$ with positive curvature until 0.02 T, followed by a gradual decrease with negative curvature for $H > 0.02$ T. Similar changes in curvature were also observed for the Tl-based tapes (Fig. 3), except for sample Tl-A in which J_c initially decreases with negative curvature before changing to positive curvature and then to negative curvature again.

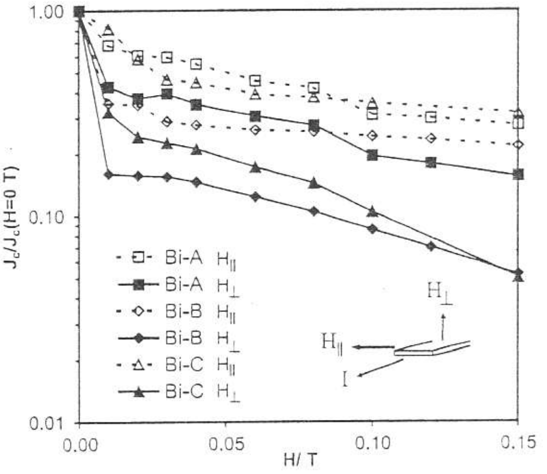

Fig. 2. Normalized J_c versus $H_\parallel$ and $H_\perp$ to the tape plane at 77 K for Bi-based tapes. I is the direction of current flow. (□) is for Bi-A with $H_\parallel$, (■) is for Bi-A with $H_\perp$, (◇) is for Bi-B with $H_\parallel$, (◆) is for Bi-B with $H_\perp$, (△) is for Bi-C with $H_\parallel$, (▲) is for Bi-C with $H_\perp$. Solid and dashed lines are a guide for the eye.

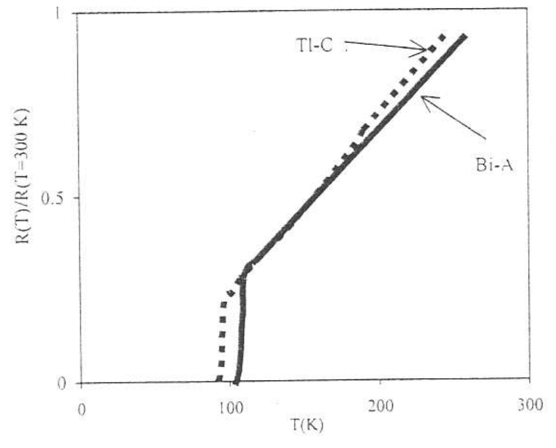

Fig. 1. Normalized electrical resistance $R(T)/R(T = 300\ \mathrm{K})$ as a function of temperature, T for samples Bi-A and Tl-C.

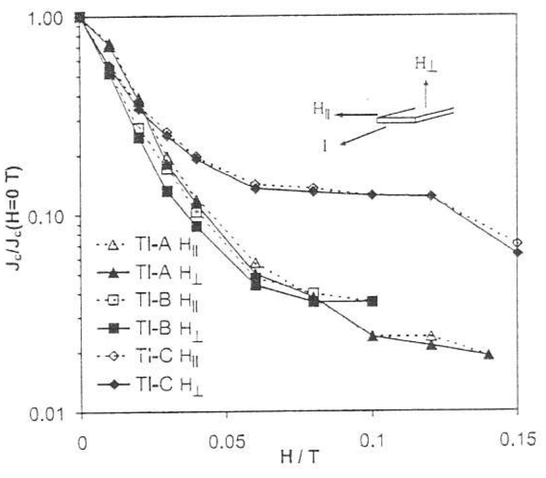

Fig. 3. Normalized J_c versus $H_\parallel$ and $H_\perp$ to the tape plane at 77 K for Tl-based tapes. I is the direction of current flow. (△) is for Tl-A with $H_\parallel$, (▲) is for Tl-A with $H_\perp$, (□) is for Tl-B with $H_\parallel$, (■) is for Tl-B with $H_\perp$, (◇) is for Tl-C with $H_\parallel$, (◆) is for Tl-C with $H_\perp$. Solid and dashed lines are a guide for the eye.

J_c of the Bi-based tapes shows an anisotropic behavior with respect to applied $H_\parallel$ and $H_\perp$ as shown in Fig. 2. The overall J_c for tapes in $H_\parallel$ are larger than J_c in $H_\perp$. This may be due to several reasons [21] such as (i) an anisotropic unit cell of Bi-2223 and Bi-2212, (ii) the existence of twist grain boundaries and residual remnant of secondary phases in the direction parallel to the tape plane, (iii) preference growth of the plate-like superconductor grains in the a–b plane direction along the tape plane as indicated in Fig. 4.

Conversely, the Tl-based tapes did not show any significant anisotropic J_c for applied $H_\parallel$ and $H_\perp$ (Fig. 3) that was observed in the Tl-1223 tape [22]. The spherical-like grains of the Tl-based tapes are randomly orientated without any alignment in certain directions as shown in Fig. 5. Unlike Bi-based tapes where the grain alignment can be accomplished by thermo-mechanical treatments, this is relatively difficult to achieve in the Tl-based tapes [14]. Therefore, the lack of grain alignment in the Tl-based tapes contributes to lower anisotropic J_c compared to the Bi-based tapes.

The degree of anisotropic transport properties as measured by anisotropy factors $(J_c(H_\perp)/J_c(H_\parallel))$ for both Bi- and Tl-based tapes are shown in Fig. 6. The value of the anisotropy factors for the Bi and Tl-based tapes are from 0.15 to 0.65 and 0.75 to 1.0, respectively. Different thermo-mechanical treatments applied to the Tl-based tapes did not result in a significant change of transport properties in applied magnetic field. For Bi-based tapes, anisotropy factors for sample Bi-A and Bi-B (subjected to intermediate rolling or sintered at longer duration) were found to be higher than the anisotropy factor for sample Bi-C. It has been shown that intermediate rolling enhances J_c following the improvement of grain-alignment along the tape plane, yet the processing condition could severely deteriorate the grain texture [23]. The in-

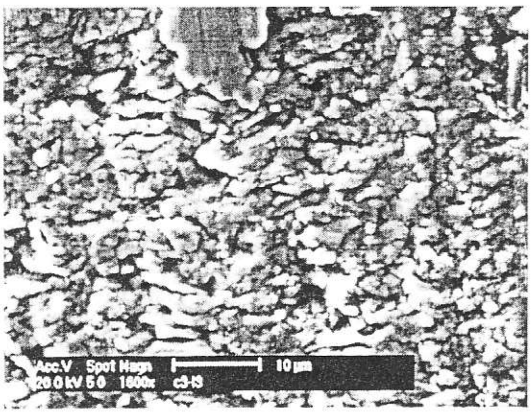

Fig. 4. SEM of sample Bi-C tapes in longitudinal cross-section showing grains aligned along the tape plane.

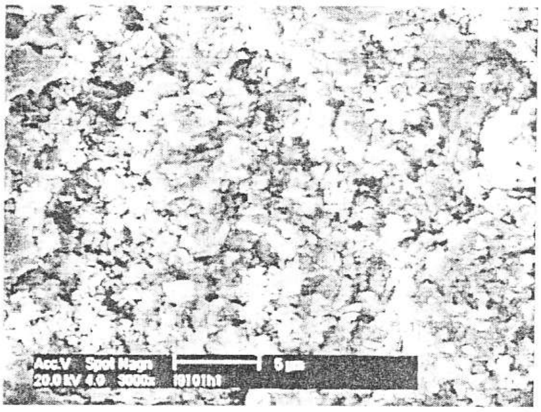

Fig. 5. SEM of sample Tl-C tapes in longitudinal cross-section showing irregular shape and sizes of grains oriented randomly along the tape plane.

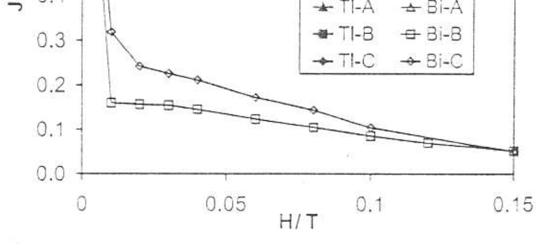

Fig. 6. Anisotropy factor for Tl- and Bi-based tapes showing the degree of anisotropy in J_c. Solid and dashed lines are a guide for the eye.

crease of the anisotropy factor for Bi-based tapes at 0.01-0.03 T may be due to a more rapid drop of J_c with applied $H_{\parallel}$ compared to applied $H_{\perp}$.

The initial decrease of J_c in low fields for either applied $H_{\parallel}$ or $H_{\perp}$ is attributed to the decoupling of Josephson weak links in the tapes [24,25]. The rapid reduction of J_c in both Bi- and Tl-based tapes shows that weak links are dominant. For Bi-based tapes, the initial decrease of J_c is only until 0.01 T. However, the initial decrease of J_c for Tl-based tapes is more gradual for both $H_{\parallel}$ and $H_{\perp}$ (up to 0.06 T), which may be due to slower decoupling of weak links. The projection of larger H on the c-axis of the Tl-based tapes is required in order to decouple almost all the weak links as clearly indicated in Fig. 7.

The supercurrent is carried mostly through strong links after the initial decrease of J_c [26–29]. By referring to the normalized J_c versus $H_{\perp}$, the percentage of strong links in the tapes was estimated from the ratio of J_c in fields to the J_c in zero field [26,27]. The amount of strong links in Tl-based tapes was found to be less than 15% of the total number of supercurrent links compared to about 20% for the Bi-based tapes. This is one of the main reasons that the J_c of the Tl-based tapes is lower than that of Bi-based tapes.The latter gradually decrease of J_c (negative curvature part as in Figs. 2 and 3 except for sample Tl-A) is ascribed to thermally activated flux creep (TAFC) [26] in the intragrains and not due to decoupling of the strong links. As reported in [30], the flux pinning strength of strong links was found to be stronger than the intragrains pinning. TAFC causes dissipation of energy and therefore suppresses J_c. From Fig. 7, J_c of the Tl-based tapes exhibits a plateau behavior for $H > 0.06$ T as the field dependence of J_c is weaker compared to the Bi-based tapes. The relatively constant J_c ($H > 0.06$ T) reflects the stronger flux pinning properties in the Tl-based tapes as a consequence of stronger interlayer coupling between adjacent Cu–O planes for the single insulating Tl–O layer of Tl-1212 materials [15,31]. The shorter spacing between the conducting Cu–O planes would reduce the anisotropy of the cell unit structure and hence lead to stronger flux pinning properties of the materials. Moreover, the pinning strength may be enhanced by small-scale defects introduced during thermo-mechanical treatments which act as pinning centers in the tape [29].

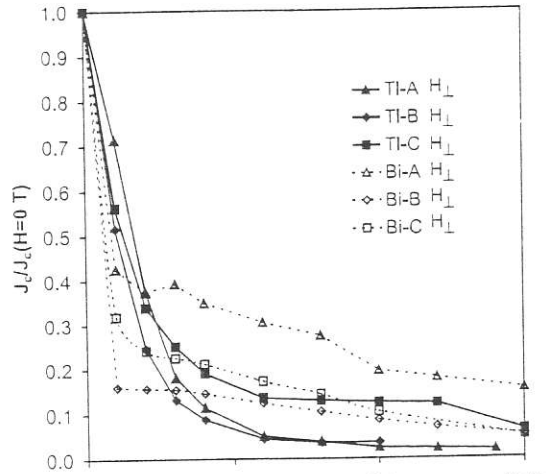

Fig. 7. Normalized J_c versus $H_{\perp}$ to the tape plane for Tl- and Bi-based tapes at 77 K. (▲) is for Tl-A with $H_{\perp}$, (◆) is for Tl-B with $H_{\perp}$, (■) is for Tl-C with $H_{\perp}$, (△) is for Bi-A with $H_{\perp}$, (◇) is for Bi-B with $H_{\perp}$, (□) is for Bi-C with $H_{\perp}$. Solid and dashed lines are a guide for the eye.

4. Conclusions

The transport critical current density of Bi-2223/Ag and Tl-1212/Ag HTSC tapes subjected to various thermo-mechanical treatments in low magnetic fields was compared. All the tapes display weak link dominated characteristics which is more severe in the Tl-1212/Ag tapes. The Bi-2223/Ag tapes show larger anisotropic transport behavior compared to Tl-1212/Ag tapes in applied field. This can be associated with the microstructural difference between these two types of tapes as revealed from SEMs. The magnetic field dependence of J_c exhibiting a plateau for $H > 0.06$ T was observed in Tl-1212/Ag tapes. This indicates the stronger flux pinning properties in Tl-1212/Ag tapes. The strong interlayer coupling that resulted reduced structural anisotropy may be responsible for the plateau in the Tl-1212/Ag tapes.

Acknowledgements

The authors are grateful to the Ministry of Science, Technology and the Environment of Malaysia for supporting this work under IRPA grant no. 09-02-02-0069.

References

[1] P. Vase, R. Flükiger, M. Leghissa, B.A. Glowacki, Supercond. Sci. Technol. 13 (2000) R71.
[2] Y. Tanaka, Physica C 335 (2000) 69.
[3] J.E. Evett, B.A. Glowacki, Supercond. Sci. Technol. 13 (2000) 443.
[4] P.F. Herrmann, J. Bock, C.-E. Bruzek, C. Cottevieille, G. Duperray, L.D. Hascicek, T. Verhaege, Y. Parasie, Supercond. Sci. Technol. 13 (2000) 477.
[5] M. Nassi, Supercond. Sci. Technol. 13 (2000) 460.
[6] K. Sato, T. Hikata, Y. Iwasa, Appl. Phys. Lett. 57 (1990) 1928.
[7] H. Kumakura, K. Togano, E. Yanagisawa, J. Kase, H. Maeda, Jpn. J. Appl. Phys. 29 (1990) L1652.
[8] S. Jin, B. van Dover, T.H. Tiefel, J.E. Graebner, N.D. Spencer, Appl. Phys. Lett. 58 (1991) 868.
[9] Z.F. Ren, J.H. Wang, Appl. Phys. Lett. 61 (1992) 1715.
[10] D.J. Miller, J.G. Hu, Z.F. Ren, J.H. Wang, J. Electron. Mater. 23 (1994) 1151.
[11] V. Selvamanickam, T. Finkle, K. Pfaffenbach, P. Haldar, E.J. Peterson, K.V. Salazaar, E.P. Roth, J.E. Tkaczyk, Physica C 260 (1996) 313.
[12] D.Y. Jeong, M.H. Sohn, H.S. Kim, L.L. He, M. Cantoni, S. Horiuchi, Physica C 269 (1996) 279.
[13] D.Y. Jeong, M.H. Sohn, Physica C 297 (1998) 192.
[14] M. Jergel, A. Conde Callardo, C. Falcony Guajardo, V. Strbík, Supercond. Sci. Technol. 9 (1996) 427.
[15] D.H. Kim, K.E. Gray, R.T. Kampwirth, J.C. Smith, D.S. Richeson, T.J. Marks, J.H. Kang, J. Talvacchio, M. Eddy, Physica C 177 (1991) 431.
[16] Z.F. Ren, J.H. Wang, Appl. Phys. Lett. 62 (1993) 3025.
[17] Z.Z. Sheng, D.X. Gu, Y. Xin, D.O. Pederson, Mod. Phys. Lett. B 5 (1991) 635.
[18] J.C. Moore, S.K. Wivell, C.H. Snowling, C.R.M. Grovenor, Physica C 235–240 (1994) 3395.
[19] R. Flükiger, B. Hensel, A. Jeremie, M. Decroux, H. Küpfer, W. Jahn, E. Seibt, W. Goldacker, Y. Yamada, J.Q. Xu, Supercond. Sci. Technol. 5 (1992) S61.
[20] D.M. Spiller, C. Beduz, Y. Yang, Y. Yi, R. Riddle, K. Pham, Physica C 235–240 (1994) 3419.
[21] B. Hensel, G. Grasso, R. Flükiger, Phys. Rev. B 51 (1995) 15456.
[22] B.A. Glowacki, S.P. Ashworth, Physica C 200 (1992) 140.
[23] T. Sakai, H. Utsunomiya, Y. Saito, T. Hanamachi, M. Shinkawa, Physica C 277 (1997) 189.
[24] J.W. Ekin, A.I. Braginski, A.J. Panson, M.A. Janocko, D.W. Capone II, N.J. Zaluzec, B. Flandermeyer, O.F. de Lima, M. Hong, J. Kwo, S.H. Liou, J. Appl. Phys. 62 (1987) 4821.
[25] J.W. Ekin, T.M. Larson, A.M. Hermann, Z.Z. Sheng, K. Togano, H. Kumakura, Physica C 160 (1989) 489.
[26] J. Horvat, S.X. Dou, H.K. Liu, R. Bhasale, Physica C 271 (1996) 51.
[27] J. Horvat, Y.C. Guo, S.X. Dou, Physica C 271 (1996) 59.
[28] D.E. Peterson, P.G. Wahlbeck, M.P. Maley, J.O. Willis, P.J. Kung, J.Y. Coulter, K.V. Salazar, D.S. Phillips, J.F. Bingert, E.J. Peterson, W.L. Hults, Physica C (1992) 161.
[29] P.J. Kung, P.G. Wahlbeck, M.E. MacHenry, M.P. Maley, D.E. Peterson, Physica C (1994) 310.
[30] N. Nakamura, G.D. Gu, K. Takamuku, M. Muarkami, N. Koshizuka, Appl. Phys. Lett. 61 (1992) 3044.
[31] S.X. Dou, H.K. Liu, Q.Y. Hu, C. Czurda, H.W. Weber, S.M. Cassidy, L.F. Cohen, A.D. Caplin, Physica B 194–196 (1994) 1829.